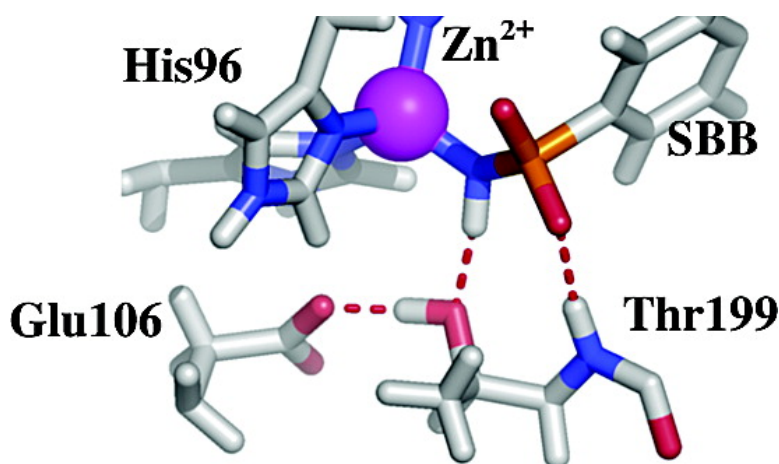Article

Pairwise Decomposition of Residue Interaction Energies Using Semiempirical Quantum Mechanical Methods in Studies of Protein–Ligand Interaction

Kaushik Raha, Arjan J. van der Vaart, Kevin E. Riley, Martin B.
Peters, Lance M. Westerhoff, Hwanho Kim, and Kenneth M. Merz

More About This Article

Additional resources and features associated with this article are available within the HTML version:

- Supporting Information
- Links to the 3 articles that cite this article, as of the time of this article download
- Access to high resolution figures
- Links to articles and content related to this article
- Copyright permission to reproduce figures and/or text from this article

View the Full Text HTML

Pairwise Decomposition of Residue Interaction Energies Using Semiempirical Quantum Mechanical Methods in Studies of Protein−Ligand Interaction

Kaushik Raha,[†,§] Arjan J. van der Vaart,[⊥] Kevin E. Riley,[†] Martin B. Peters,[†] Lance M. Westerhoff,[†,‡] Hwanho Kim,[‡] and Kenneth M. Merz, Jr.*,[†]

Contribution from the Department of Chemistry, 104 Chemistry Building, The Pennsylvania State University, University Park, Pennsylvania 16802, QuantumBio, Inc., State College, Pennsylvania 16803, and Integrative Biosciences Graduate Program, The Huck Institute of Life Sciences, The Pennsylvania State University, University Park, Pennsylvania 16802

Received December 6, 2004; E-mail: merz@psu.edu

Abstract: Pairwise decomposition of the interaction energy between molecules is shown to be a powerful tool that can increase our understanding of macromolecular recognition processes. Herein we calculate the pairwise decomposition of the interaction energy between the protein human carbonic anhydrase II (HCAII) and the fluorine-substituted ligand *N*-(4-sulfamylbenzoyl)benzylamine (SBB) using semiempirical quantum mechanics based methods. We dissect the interaction between the ligand and the protein by dividing the ligand and the protein into subsystems to understand the structure−activity relationships as a result of fluorine substitution. In particular, the off-diagonal elements of the Fock matrix that is composed of the interaction between the ionic core and the valence electrons and the exchange energy between the subsystems or atoms of interest is examined in detail. Our analysis reveals that the fluorine-substituted benzylamine group of SBB does not directly affect the binding energy. Rather, we find that the strength of the interaction between Thr199 of HCAII and the sulfamylbenzoyl group of SBB affects the binding affinity between the protein and the ligand. These observations underline the importance of the sulfonamide group in binding affinity as shown by previous experiments (Maren, T. H.; Wiley: C. E. *J. Med. Chem.* **1968**, *11*, 228−232). Moreover, our calculations qualitatively agree with the structural aspects of these protein−ligand complexes as determined by X-ray crystallography.

Introduction

Obtaining molecular- or atomic-level insights into the energy of interaction between a protein and a ligand by experimental methods remains a significant challenge. Experimental studies generally report macroscopic dissociation or an inhibition constant that relates to the free energy of binding between the participating species, such as a protein and a ligand in the condensed phase.[2] The attribution or partitioning of the free energy of binding to different parts of the molecules such as residues, side chains, or backbone atoms in the protein and core or branch groups on the ligand can be achieved through experimental methods by engineering mutations into the protein or synthesis of an altered ligand with or without certain functional groups. Large-scale structure−activity studies using combinatorial chemistry are often used where the chemical space

accessible to the ligand is explored by brute force.[3,4] Thermodynamic double mutant cycles and pH titration or pK_a based approaches are traditionally used to experimentally measure the electrostatic interaction energy between charged groups in protein−ligand complexes.[5,6] While possible, such approaches are expensive both in terms of time and resources.

pK_a approaches maintain the structural integrity and measure the free energy of charging ionizable groups in a protein environment but neglect the desolvation and background interactions of the ionizable groups. Thermodynamic double mutant cycles are invasive methods in which desolvation and environment-dependent changes are assumed to cancel out due to the double mutant cycle.[7] These assumptions are difficult to test rigorously, and moreover, mutations or synthetically altered ligands might cause unanticipated structural changes[8] that affect the ability of a protein to recognize a small-molecule ligand.

[†] Department of Chemistry, 104 Chemistry Building, The Pennsylvania State University.

[‡] QuantumBio, Inc.

[§] Integrative Biosciences Graduate Program, The Huck Institute of Life Sciences, The Pennsylvania State University.

[⊥] Present address: Department of Chemistry and Chemical Biology, Harvard University, Cambridge, MA 02138.

(1) Maren, T. H.; Wiley: C. E. *J. Med. Chem.* **1968**, *11*, 228−232.
(2) Ajay; Murcko, M. A. *J. Med. Chem.* **1995**, *38*, 4953−4967.
(3) Garg, R.; Kurup, A.; Mekapati, S. B.; Hansch, C. *Chem. Rev.* **2003**, *103*, 703−732.
(4) Kassel, D. B. *Chem. Rev.* **2001**, *101*, 255−268.
(5) Roth, T. A.; Minasov, G.; Morandi, S.; Prati, F.; Shoichet, B. K. *Biochemistry* **2003**, *42*, 14483−14491.
(6) Robinson, C. R.; Sligar, S. G. *Protein Sci.* **1993**, *2*, 826−837.
(7) Bosshard, H. R.; Marti, D. N.; Jelesarov, I. *J. Mol. Recognit.* **2004**, *17*, 1−16.
(8) Ma, B.; Shatsky, M.; Wolfson, H. J.; Nussinov, R. *Protein Sci.* **2001**, *11*, 184−197.

Protein targets that recognize small-molecule ligands have conserved residues that are essential for its function as an enzyme. Examples of such residues are the catalytic dyad of Asp residues in aspartyl proteases, the catalytic triad of Ser, His, and Asp in serine proteases, and the zinc-coordinating His residues in metalloenzymes such as human carbonic anhydrase and matrix metalloproteases.[9] Critical interactions between functional groups of conserved residues and bound ligands are very challenging to estimate using experimental methods because mutation of these residues often leads to loss of interaction between the ligand and the protein.[10,11] Also, although ligands are expected to bind to the active site of the enzyme under consideration, often some ligands bind to an alternate site, leading to disruption of the active site of the protein. This phenomenon known as allosteric inhibition has also been reported in the literature.[12,13]

Hence, there is no direct and unambiguous experimental approach to assess the strength of interaction between different parts of a small molecule and its host from its structure. Indeed, changes made in a ligand are either through brute-force combinatorial approaches or through a more rational approach based on visual inspection of an experimentally determined structure and/or via chemical intuition. From a computational perspective, this problem easily lends itself to an energy decomposition of residue or ligand fragment interactions, which are greatly facilitated when the energy functions used are pairwise additive.

Potential functions or "scoring functions" used to assess protein−ligand interactions are, in many instances, molecular mechanics (MM) based potentials[14−16] that are pairwise additive and lend themselves to the execution of pairwise energy decomposition analyses to determine intra- and intermolecular interaction energies. Thus, energy decomposition using these potentials is fairly straightforward if the force field parameters are available. However, the problem often arises due to the accuracy of these potentials and their ability to reliably predict the strength of the binding free energy. This is even more important when metals are involved in the recognition process.[17] Moreover, most of these potentials are formulated in such a way that polarization or charge-transfer effects are incorporated in, at best, an average way. Hence, validation of such potentials in energy decomposition analyses becomes critical before any conclusions can be drawn from such an analysis.

Quantum mechanics (QM) methods are physically based, and they rely on a fundamentally different approach in which the Schrödinger equation is solved and molecular properties are calculated from the wave function. Until recently, these methods were applicable to "small" molecules, but with the advent of linear scaling methods its has become possible to routinely study
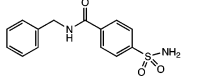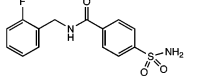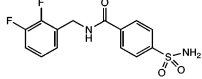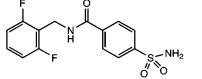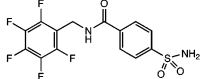
biological macromolecules such as proteins and nucleic acids.[18−21] In recent work from our group we have reported the development of a linear scaling methodology that uses the divide and conquer (D&C) approach for solving large molecular systems with QM.[18,22] This method has been implemented in the computer program DivCon[23] which uses the semiempirical Hamiltonians such as AM1,[24] PM3,[25] MNDO/d,[26,27] or PM3-PDDG[28] to solve the Schrödinger equation for large biomolecular systems. This family of semiempirical methods is based on the neglect of diatomic differential overlap (NDDO) formalism which reduces the computational cost by neglecting certain interactions and fitting others to experimental data.[29,30] These methods have been used to model biomolecular solvation[31,32] and chemical reactivity,[33,34] calculate binding free energy in protein−ligand interaction,[35,36] and predict NMR chemical shifts from the three-dimensional structure of protein−ligand complexes.[37] The use of NDDO formalism also permits the partitioning of the electrostatic energy into self- and cross components between atoms or residues.[38] This allows for the analysis of electrostatic interactions between, for example, the residues of a protein and groups in a small-molecule ligand to estimate their contribution to the binding affinity.

In this study, we present a pairwise decomposition scheme for evaluating the electrostatic interaction energy using what we will term as the neglect of nonbonded differential overlap (NNDO) formalism that can be applied to study protein−ligand interaction via our linear-scaling D&C technology. This scheme permits the calculation of the self-energy of the atom, core−electron interactions, electron−electron repulsion, and exchange between atoms from the molecular electron density. We also demonstrate the utility of this method by analyzing the structure−activity relationships in a set of fluorine-substituted *N*-(4-sulfamylbenzoyl)benzylamine (SBB: for structures see Table 1) inhibitors bound to human carbonic anhydrase II (HCAII). HCAII is a zinc metalloenzyme that catalyzes the hydration of carbon dioxide, releasing bicarbonate and a proton. Inhibition of HCAII is of clinical importance and can be useful

(9) Babine, R. E.; Bender, S. L. *Chem. Rev.* **1997**, *87*, 1359−1472.
(10) Eaazhisai, K.; Balaram, H.; Balaram, P.; Murthy, M. R. *J. Mol. Biol.* **2004**, *343*, 671−684.
(11) Gutteridge, A.; Thornton, J. M. *FEBS Lett.* **2004**, *567*, 67−73.
(12) Horn, J. R.; Shoichet, B. K. *J. Mol. Biol.* **2004**, *336*, 1283−1291.
(13) Esnouf, R.; Ren, C.; Ross, Y.; Jones, D.; Stammers, D.; Stuart, D. *Nat. Struct. Biol.* **1995**, *2*, 303−308.
(14) Cornell, W. D.; Cieplak, P.; Bayly, C. I.; Gould, I. R.; Merz, K. M., Jr.; Ferguson, D. M.; Spellmeyer, D. C.; Fox, T.; Caldwell, J. W.; Kollman, P. A. *J. Am. Chem. Soc* **1995**, *117*, 5179−5197.
(15) Brooks, B. R.; Bruccoleri, R. E.; Olafson, B. D.; States, D. J.; Swaminathan, S.; Karplus, M. *J. Comput. Chem.* **1983**, *4*, 182−217.
(16) Jorgensen, W. L.; Maxwell, D. S.; Tirado-Rives, J. *J. Am. Chem. Soc.* **1996**, *118*, 11225−11236.
(17) Raha, K.; Merz, K. M., Jr. *Ann. Rep. Comput. Chem.* **2004**. In press.

(18) Dixon, S. L.; Merz, K. M., Jr. *J. Chem. Phys.* **1997**, *107*, 879−893.
(19) van der Vaart, A.; Gogonea, V.; Dixon, S. L.; Merz, K. M., Jr. *J. Comput. Chem.* **2000**, *21*, 1494−1504.
(20) Khandogin, J.; York, D. M. *Proteins: Struct. Funct. Bioinfor.* **2004**, *56*, 724−737.
(21) Yang, W.; Lee, T.-S. *J. Chem. Phys.* **1995**, *103*, 5674−5678.
(22) Dixon, S. L.; Merz, K. M., Jr. *J. Chem. Phys.* **1996**, *104*, 6643−6649.
(23) Dixon, S. L.; van der Vaart, A.; Gogonea, V.; Vincent, J. J.; Brothers, E. N.; Suárez, D.; Westerhoff, L. M.; Merz, K. M., Jr. The Pennsylvania State University, 1999.
(24) Dewar, M. J. S.; Zoebisch, E. G.; Healy, E. F.; Stewart, J. J. P. *J. Am. Chem. Soc.* **1985**, *107*, 3902−3909.
(25) Cramer, C. J.; Truhlar, D. G. *J. Comput. Chem.* **1992**, *12*, 1089−1097.
(26) Dewar, M. J. S.; Thiel, W. *J. Am. Chem. Soc.* **1977**, *99*, 4899−4907.
(27) Thiel, W.; Voityuk, A. A. *J. Phys. Chem.* **1996**, *100*, 616−626.
(28) Repasky, M. P.; Chandrasekhar, J.; Jorgensen, W. L. *J. Comput. Chem.* **2002**, *23*, 1601−1622.
(29) Stewart, J. J. P.; Lipkowitz, K. B., Boyd, D. B., Eds. VHC: New York, 1990; Vol. 2, pp 313−365.
(30) Zerner, M. C.; Lipkowitz, K. B., Boyd, D. B., Eds. VHC: New York, 1991; Vol. 2.
(31) Gogonea, V.; Merz, K. M., Jr. *J. Phys. Chem. A* **1999**, *103*, 5171−5188.
(32) Gogonea, V.; Merz, K. M., Jr. *J. Phys. Chem. B* **2000**, *104*, 2117−2122.
(33) Diaz, N.; Sordo, T. L.; Merz, K. M., Jr.; Suarez, D. *J. Am. Chem. Soc.* **2003**, *125*, 672−684.
(34) Suarez, D.; Merz, K. M., Jr. *J. Am. Chem. Soc.* **2001**, *123*, 3759−3770.
(35) Raha, K.; Merz, K. M., Jr. *J. Am. Chem. Soc.* **2004**, *126*, 1020−1021.
(36) Nikitina, E.; Sulimov, D.; Zayets, V.; Zaitseva, N. *Int. J. Quant. Chem.* **2004**, *97*, 747−763.
(37) Wang, B.; Raha, K.; Merz, K. M., Jr. *J. Am. Chem. Soc.* **2004**, *126*, 11430−11431.
(38) Curutchet, C.; Salichs, A.; Barril, X.; Orozco, M.; Luque, F. J. *J. Comput. Chem.* **2002**, *24*, 32−45.

Table 1. Five *N*-(4-Sulfamylbenzoyl)benzylamine (SBB)-Based Inhibitors Listed by Binding Free Energy to HCAII and Associated PDB ID[a]

| Inhibitor	ΔG_{bind} Wild type (kcal/mol)	ΔG_{bind} F131V (kcal/mol)	PDB ID Wild type	PDB ID F131V
4-(aminosulfonyl)-N-phenylmethyl-benzamide (SBB)	-11.80	-11.22		1G40
4-(aminosulfonyl)-N-[(2-fluorophenyl)methyl]-benzamide (2-fluoro-SBB)	-12.84	-11.75	1G1D	1G45
4-(aminosulfonyl)-N-[(2,3-difluorophenyl)methyl]-benzamide (2,3-difluoro-SBB)	-12.97	-11.96	1G52	1G46
4-(aminosulfonyl)-N-[(2,6-difluorophenyl)methyl]-benzamide (2,6-difluoro-SBB)	-12.30	-11.44	1G53	1G48
4-(aminosulfonyl)-N-[(2,3,4,5,6-pentaflurophenyl)methyl]-benzamide (pentafluoro-SBB)	-12.00	-11.83	1G54	1G4J

[a] For SBB complexed with wild-type HCAII, fluorine was substituted by hydrogen in 2-fluoro-SBB extracted from 1G1D.

in treatment of numerous diseases such as glaucoma.[39] The active site of the enzyme contains a zinc atom, which is tetrahedrally coordinated by three histidine residues. In the free state, a water molecule, presumably present as the hydroxyl ion (OH$^-$), coordinates the zinc.[40] Most potent inhibitors of HCAII have a terminal sulfonamide group that coordinates the zinc atom, bonded to an aromatic group[41,42] (Figure 1).

The acidic character of the sulfonamide group has been shown to have a major influence on the binding affinity of this class of inhibitors.[1] One of the sulfonamide oxygen atoms interacts with Thr199 of the enzyme, which is a key catalytic residue. The SBB inhibitors also have a sulfonamide moiety bonded to an aromatic group and are nanomolar inhibitors of HCAII. We chose the SBB inhibitors for a pairwise decomposition analysis because of the following reasons: (1) High-resolution X-ray crystal structures of the fluorine-substituted inhibitors bound to wild-type HCAII and the F131V mutant were available in the protein databank (PDB).[43] (2) The inhibition constants of the inhibitors bound to HCAII and the mutant F131V measured by Kim et al. under the same conditions of pH and temperature are available in the literature.[44] (3) The electronic nature of the active site and inhibitors makes this system well suited for QM

pairwise decomposition analysis because MM potentials would likely have difficulty characterizing these interactions because QM features such as polarization or charge transfer may play a role.

The substitution of fluorine atoms on the benzyl group of SBB modifies the electronic character of the aromatic ring and influences an edge-to-face interaction between Phe131 and the benzyl group of SBB. As discussed[44] by Kim et al. in detail, this is an example of a quadrupole−quadrupole interaction in which the partial positive charge on the ring hydrogen of Phe131 interacts favorably with the partial negative charge above the aromatic group of the inhibitor. This quadrupole−quadrupole interaction is not associated with the atomic nucleus but with the molecular charge distribution and is referred to as molecular electric quadrupole moments.[45] Williams et al. discuss the importance of the molecular electric quadrupole moments in aromatic compounds such as benzene (C_6H_6) and hexafluoro-benzene (C_6F_6) in determining their solid-state architecture. In similar quadrupolar molecules such as benzene or hexafluoro-benzene the edge-to-face or T-shaped orientation maximizes the electrostatic attraction, whereas for a binary mixture such as C_6H_6/C_6F_6 a linear stacked interaction where a benzene quadrupole moment is stacked parallel to hexafluorobenzene quadrupole moment maximizes electrostatic attraction.[45] The quadrupole in benzene is topologically similar to a d_{z^2} orbital,[46] and the T-shaped interaction can be schematically represented as:
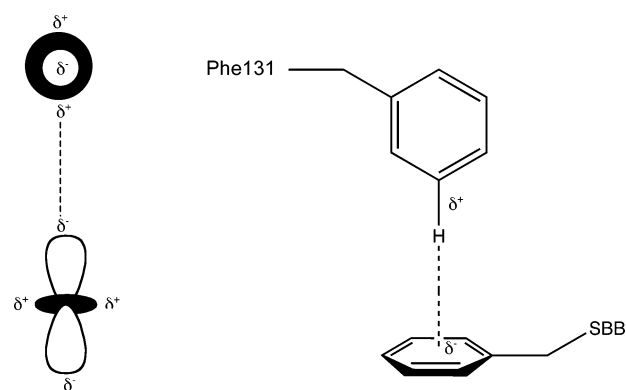
When fluorine is substituted on the aromatic ring, the negative character of the charge above the ring diminishes, thereby leading to a less attractive interaction between the two. However, disruption of this interaction by fluorination is apparently favorable toward binding as evidenced by the binding affinities of the fluorine-substituted SBB inhibitors (Table 1). The structural aspects of the interaction between Phe131 and fluorinated SBB derivatives are counterintuitive since with the disruption of a classical quadrupole−quadrupole interaction it is expected that the distance between the benzyl group and Phe131 would increase due to the *less attractive* interaction between the partial positive charge on the ring hydrogen of Phe131 and the diminished negative charge above the aromatic ring. What is seen in the X-ray crystal structures, instead, is this distance, as measured between the centroid of Phe131 and the benzyl ring of SBB, decreasing in the fluorinated benzyl groups (Table 2).[44] Kim et al. suggest that the quadrupole−

(39) Surgrue, M. F. *Prog. Retinal Eye Res.* **2000**, *19*, 87−112.
(40) Merz, K. M., Jr.; Banci, L. *J. Am. Chem. Soc.* **1997**, *119*, 863−871.
(41) Christianson, D. W.; Fierke, C. A. *Acc. Chem. Res* **1996**, *29*, 331−339.
(42) Gruneberg, S.; Stubbs, M. T.; Klebe, G. *J. Med. Chem.* **2002**, *45*, 3588−3602.
(43) Berman, H. M.; Westbrook, J.; Feng, Z.; Gilliland, G.; Bhat, T. N.; Weissig, H.; Shindyalov, I. N.; Bourne, P. E. *Nucleic Acids Res.* **2000**, *28*, 235−242.
(44) Kim, C. Y.; Chang, J. S.; Doyon, J. B.; Baird, T. T., Jr.; Fierke, C. A.; Jain, A.; Christianson, D. W. *J. Am. Chem. Soc.* **2000**, *122*, 12125−12134.

(45) Williams, J. H. *Acc. Chem. Res.* **1993**, *26*, 593−598.
(46) Ma, J. C.; Dougherty, D. A. *Chem. Rev.* **1997**, *97*, 1303−1324.

Table 2. Pairwise Interaction (PW$_{int}$) between Phe131 and SS3 of SBB; (B) Interaction Energy between Geometry Optimized Benzene- and Fluorine-Substituted Benzene Dimers Calculated Using the Hartree−Fock (HF) Method with the 6-31+G* Basis Set

(A)

complex	$\Delta G_{exp}{}^a$ (kcal/mol)	Phe-131 SS3 distance^b (Å)	PW$_{int}$ AM1^c (kcal/mol)	PW$_{int}$ Coulombic^d (kcal/mol)	PW$_{int}$ PM3^e (kcal/mol)	PW$_{int}$ Coulombic (kcal/mol)
native−SBB	−11.80	5.92	−0.22	−0.02	−0.83	−0.05
native−2-fluoro-SBB	−12.84	5.95	−0.21	0.00	−0.82	−0.04
native−2,3-difluoro-SBB	−12.97	5.51	−0.37	0.04	−1.2	−0.02
native−2,6-difluoro-SBB	−12.30	6.76	−1.81	0.03	−4.2	−0.01
native−2,3,4,5,6-pentafluoro-SBB	−12.00	5.08	−1.30	0.21	−3.4	0.15

(B)

dimer^f	ΔE_I (HF) (kcal/mol)	ΔH_I (AM1) (kcal/mol)	ΔH_I (PM3) (kcal/mol)	intercentroid distance (Å)
benzene−benzene	−0.33	−0.08	−0.16	6.12
benzene−2-fluoro-benzene	−0.20	−0.01	−0.14	5.96
benzene−2,3-difluoro-benzene	−0.12	0.04	−0.11	5.95
benzene−2,6-difluoro-benzene	−0.01	0.06	−0.05	6.09
benzene−2,3,4,5,6-pentafluoro-SBB	0.30	0.31	0.07	5.82

^{a} ΔG_{exp} for SBB inhibitors binding to HCAII is given in kcal/mol. ^{b} Distance is measured in Å between the centroids of Phe131 and SS3. ^{c} PW$_{int}$ is calculated using the AM1 and PM3 Hamiltonians. ^{c} Coulombic PW$_{int}$ is calculated from CM2 charges calculated using AM1 and PM3 Hamiltonian with DivCon/PB-SCRF method. ^{e} PW$_{int}$ between Val 131 and SS3 in F131V HCAII is calculated to be zero and, hence, is not shown. ^{f} Single-point calculations were performed on HF geometries with the semiempirical methods using the AM1 and PM3 Hamiltonians.
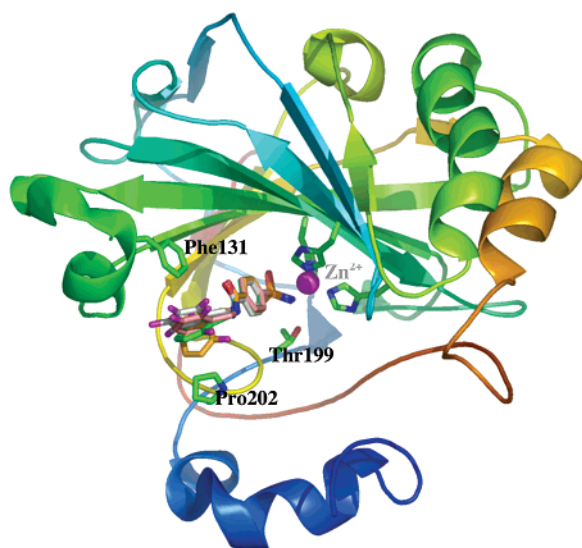

Figure 1. Fluorinated *N*-(4-sulfamylbenzoyl)benzylamine (SBB) inhibitors bound to human carbonic anhydrase II (HCAII). Residues Phe131 and Pro202, of HCAII interacting with aromatic group of SBB inhibitors are depicted. Fluorine substitution disrupts edge-to-face interaction between Phe131 and aromatic ring of SBB inhibitors. Residue Thr199, interacting with the sulfonamide group of each SBB inhibitor, is also depicted here.

quadrupole interaction is less significant than other factors such as optimization of van der Waals contact surface for the fluoroaromatic rings in this case.

To further probe this interaction Kim et al. mutated Phe131 to a valine (F131V) and experimentally obtained the inhibition constants and X-ray crystal structures of SBB inhibitors bound to mutant F131V HCAII. The SBB inhibitors bound to F131V are 1−6 times less potent than when bound to the wild-type HCAII enzyme. These observations underscore the importance of this interaction; however, visual inspection of the crystal structures of SBB inhibitors with F131V reveals that the fluoroaromatic rings in response to the mutation rotate about the C-phenyl bond (Figure 2b). Another key interaction pair

between HCAII inhibitors and the enzyme is Thr199 and the sulfonamide group, which has been characterized as a key mediator influencing inhibitor binding affinity.[1] The nitrogen of the sulfonamide group acts as a hydrogen bond donor to the hydroxyl group of Thr199, and one of the sulfonamide oxygen atoms acts as a hydrogen bond acceptor from the backbone NH group. Because the hydroxyl group of the Thr199 side chain accepts a hydrogen bond from the zinc-bound hydroxyl ion during catalysis, Thr199 has been labeled as a "doorkeeper" to catalysis.[41,47]

In this work we use a semiempirical QM level of theory and a pairwise decomposition scheme to probe these unusual structure−activity relationships between different groups of SBB inhibitors and the HCAII enzyme with an aim toward gaining a deeper understanding of molecular recognition and the inhibition process.

Theoretical Background and Computational Details

For single determinant wave functions, the electronic energy (E_{el}) is given by:

$$E_{el} = \frac{1}{2}\sum_{\mu\nu}P_{\mu\nu}(H + F)_{\nu\mu} \qquad (1)$$

where P is the density matrix, H the one-electron matrix, and F the Fock matrix. The Fock matrix is given by:

$$F_{\mu\nu} = H_{\mu\nu} + \sum_{\lambda\sigma}P_{\lambda\sigma}\left[(\mu\nu|\sigma\lambda) - \frac{1}{2}(\mu\sigma|\lambda\nu)\right] \qquad (2)$$

where $(\mu\nu|\sigma\lambda)$ are the two electron integrals. The basis functions can now be grouped, based on which atoms they are centered. Since P, H,

(47) Hakansson, K.; Carlsson, M.; Svensson, L. A.; Liljas, A. *J. Mol. Biol.* **1992**, *227*, 1192−1204.

and F are symmetric, this gives the following identities:

$$\sum_\mu = \sum_A^{} \sum_\mu^A \tag{3}$$

$$\frac{1}{2}\sum_{\mu\nu} = \frac{1}{2}\sum_A^{}\sum_\mu^A\left\{\sum_\nu^A + \sum_{B\neq A}^{}\sum_\nu^B\right\} = \frac{1}{2}\sum_A^{}\sum_\mu^A\left\{\sum_\nu^A + 2\sum_{B<A}^{}\sum_\nu^B\right\} \tag{4}$$

$$\sum_{\lambda\sigma} = \sum_{\lambda\sigma}^A + \sum_{B\neq A}^{}\sum_\lambda^A\sum_\sigma^B + \sum_{B\neq A}^{}\sum_\lambda^B\sum_\sigma^A + \sum_{B\neq A}^{}\sum_{\lambda\sigma}^B$$
$$= \sum_{\lambda\sigma}^A + 2\sum_{B<A}^{}\sum_\lambda^A\sum_\sigma^B + 2\sum_{B<A}^{}\sum_\lambda^B\sum_\sigma^A + 2\sum_{B<A}^{}\sum_{\lambda\sigma}^B \tag{5}$$

where the short hand notation

$$\sum_A^{}$$

means summation over all atoms A, and

$$\sum_\mu^A$$

means summation over all functions μ that are centered on atom A (that is,

$$\sum_\mu^A \equiv \sum_{\mu \in A}$$

Now, substituting eq 2 into 1 and grouping the basis functions by atomic centers (eqs 3−5), subject to the NDDO approximation yields:

$$\text{NDDO:}\quad (\mu^A\nu^B|\sigma^C\lambda^D) = (\mu^A\nu^A|\sigma^C\lambda^C)\delta_{AB}\delta_{CD} \tag{6}$$

where δ_{AB} is the Krönecker delta function. This gives:

$$E_{\text{el}} =$$
$$\frac{1}{2}\sum_A^{}\sum_\mu^A\left\{\begin{array}{l}\sum_\nu^A P_{\mu\nu}{}^{AA}\left(2H_{\mu\nu}{}^{AA} + \sum_{\lambda\sigma}^{}P_{\lambda\sigma}\left[(\mu^A\nu^A|\sigma\lambda) - \frac{1}{2}(\mu^A\sigma|\lambda\nu^A)\right]\right) \\ + 2\sum_{B<A}^{}\sum_\nu^B P_{\mu\nu}{}^{AB}\left(2H_{\mu\nu}{}^{AB} - \frac{1}{2}\sum_{\lambda\sigma}^{}P_{\lambda\sigma}(\mu^A\sigma|\lambda\nu^B)\right)\end{array}\right\} \tag{7}$$

where μ^A indicates that μ is centered on atom A, and $X_{\mu\nu}{}^{AB} \equiv X_{\mu\nu}$ with $\mu \in A$, $\nu \in B$ and $X = H,P$. Further grouping leads to:

$$E_{\text{el}} = \frac{1}{2}\sum_A^{}\sum_\mu^A$$
$$\left\{\begin{array}{l}\left[\sum_\nu^A P_{\mu\nu}{}^{AA}\left(2H_{\mu\nu}{}^{AA} + \sum_{\lambda\sigma}^A P_{\lambda\sigma}{}^{AA}\left[(\mu^A\nu^A|\sigma^A\lambda^A) - \frac{1}{2}(\mu^A\sigma^A|\lambda^A\nu^A)\right] + \right. \right. \\ \left. \left. 2\sum_{B<A}^{}\sum_{\lambda\sigma}^B P_{\lambda\sigma}{}^{BB}(\mu^A\nu^A|\sigma^B\lambda^B)\right)\right] \\ + 2\sum_{B<A}^{}\sum_\nu^B P_{\mu\nu}{}^{AB}\left(2H_{\mu\nu}{}^{AB} - \frac{1}{2}\sum_\lambda^B\sum_\sigma^A P_{\lambda\sigma}{}^{BA}(\mu^A\sigma^A|\lambda^B\nu^B)\right)\end{array}\right\} \tag{8}$$

Grouping all terms that depend on A only, and all terms that depend both on A and B, we can now write

$$E = E_{\text{el}} + E_{\text{core}} = \sum_A^{}\left\{E_A + \sum_{B<A}^{}(E'_{AB} + E_{AB} + E_{\text{core}AB})\right\} \tag{9}$$

where E is the total energy, and

$$E_A =$$
$$\frac{1}{2}\sum_\mu^A\sum_\nu^A P_{\mu\nu}{}^{AA}\left(2H_{\mu\nu}{}^{AA} + \sum_{\lambda\sigma}^A P_{\lambda\sigma}{}^{AA}\left[(\mu^A\nu^A|\sigma^A\lambda^A) - \frac{1}{2}(\mu^A\sigma^A|\lambda^A\nu^A)\right]\right) \tag{10}$$

$$E'_{AB} = \sum_\mu^A\sum_\nu^A\sum_{\lambda\sigma}^B P_{\mu\nu}{}^{AA}P_{\lambda\sigma}{}^{BB}(\mu^A\nu^A|\sigma^B\lambda^B) \tag{11}$$

$$E_{AB} = \sum_\mu^A\sum_\nu^B P_{\mu\nu}{}^{AB}\left(2H_{\mu\nu}{}^{AB} - \frac{1}{2}\sum_\lambda^B\sum_\sigma^A P_{\lambda\sigma}{}^{BA}(\mu^A\sigma^A|\lambda^B\nu^B)\right) \tag{12}$$

and $E_{\text{core}AB}$ the core−core repulsion between atoms A and B. Equations 9−12 constitute the pairwise energy decomposition, which is general for NDDO-type methods. The preceding theoretical framework for the neglect of nonbonded differential overlap (NNDO) formalism can be applied to study intermolecular interactions, but specifically we focus herein on protein−ligand interactions using a combination of NNDO and our linear-scaling D&C technology. Fischer and Kollmar,[48] first derived the formalisms for decomposing semiempirical energy into pairwise contributions. In later studies Dewar and Lo[49] and Olivella and Vilarrasa[50] applied energy partitioning schemes to the MINDO/2 and MNDO methods to study the Cope rearrangement and the basicity of azole-based compounds.

Unfortunately, the decomposition is not strictly pairwise, because of the E_A term. This energy stems from the diagonal blocks of the Fock, one-electron, and density matrixes. E_A can be interpreted as the "self" energy of the atom at the molecular electron density. We note that this does not mean that E_A is a constant independent of the other atoms: the electron density around atoms ($P_{\mu\nu}{}^{AA}$ and $P_{\lambda\sigma}{}^{AA}$) are implicit functions of the total electron density ($P_{\mu\nu}{}^{AA}$ and $P_{\lambda\sigma}{}^{AA}$ are only elements of the density matrix; the total density matrix has been obtained in a self-consistent iterative process for the *whole* system). E_A will change from system to system and from configuration to configuration. Moreover, E_A has a large and negative energy contribution, since the one-electron terms contained in it are large and negative (in fact, E_A contains most of the energy of the system). E'_{AB} comes from the diagonal block of the Fock matrix. It contains all electron repulsion between atoms A and B and is therefore always positive. E_{AB} comes from the off-diagonal matrix elements. It contains the exchange between the atoms and the one-electron matrix elements and is therefore negative. E_{AB} contains most of the binding energy.

Equations 12−15 can also be used to decompose the interaction energy (E_{int}), the electrostatic (E_{es}), polarization (E_{pol}) and charge transfer (E_{CT}) energies into pairwise atomic interactions. These energies are given by[51]

$$E_{\text{int}} = E[\epsilon_{\text{F}},P_r,r,b] - E[(\epsilon_p,\epsilon_w),P_\infty,\infty,0] \tag{13}$$

$$E_{\text{es}} = E[(\epsilon_p,\epsilon_w),P_\infty,r,0] - E[(\epsilon_p,\epsilon_w),P_\infty,\infty,0] \tag{14}$$

$$E_{\text{pol}} = E[(\epsilon_p,\epsilon_w),P'_r,r,0] - E[(\epsilon_p,\epsilon_w),P_\infty,r,0] \tag{15}$$

$$E_{\text{CT}} = E[\epsilon_{\text{F}},P_r,r,b] - E[(\epsilon_p,\epsilon_w),P'_r,r,0] \tag{16}$$

where ϵ_{F} is the Fermi energy of the entire system, ϵ_p and ϵ_w the Fermi energies of the interacting subsystems, b is the subsystem overlap vector, r the distance between the subsystems and P_r the density matrix at
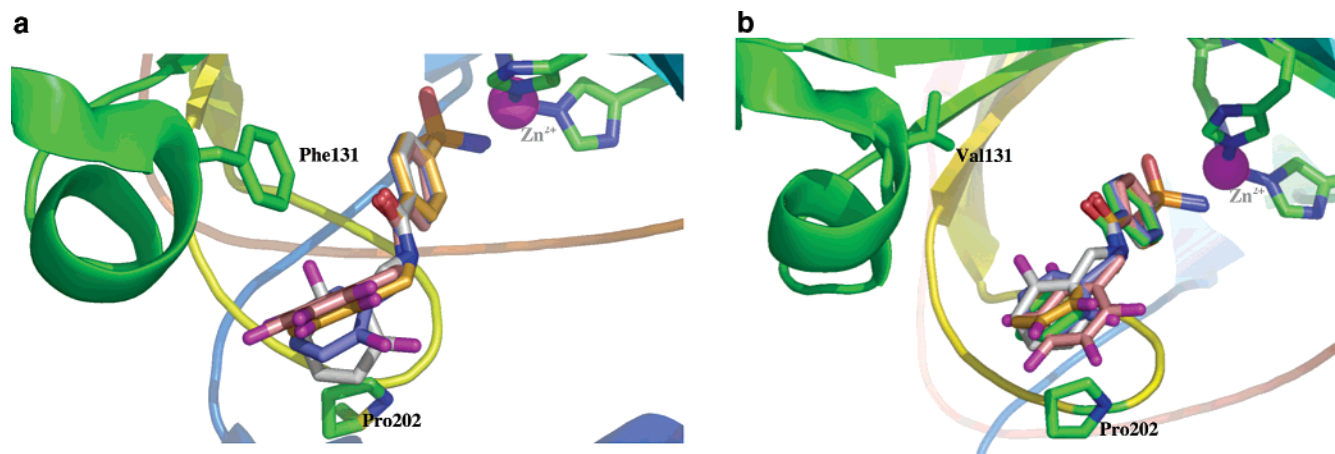
a

b

Figure 2. (a) Snapshot of SBB inhibitors bound to HCAII and interacting with Phe131 and Pro202 residues. The distances between the centroids of Phe131 and the aromatic rings of SBB inhibitors shown here are listed in Table 2. The distances between the centroids of Pro202 and the aromatic rings of SBB inhibitors shown here are listed in Table 4. Color code, **violet**: 2-fluoro-SBB, **orange**: 2,3-difluoro-SBB, **white**: 2,6-difluoro-SBB, **salmon**: 2,3,4,5,6-pentafluoro-SBB. 2,6-difluoro-SBB (white) disrupts the edge-to-face interaction between Phe131 and the aromatic ring. In all inhibitors, purple: fluorine, red: oxygen, blue: nitrogen. (b) Snapshot of SBB inhibitors bound to F131V HCAII and interacting with Val131 and Pro202 residues. The distances between centroids of Pro202 and the aromatic rings of SBB inhibitors shown here are listed in Table 4. The distances between the centroids of Val131 and aromatic rings of SBB inhibitors shown here are listed with the color code of the inhibitors as follows: **green**: SBB (8.55 Å), **violet**: 2-fluoro-SBB (8.39 Å), **orange**: 2,3-difluoro-SBB (8.18 Å), **white**: 2,6-difluoro-SBB (8.04 Å), **salmon**: 2,3,4,5,6-pentafluoro-SBB (8.94 Å). In all inhibitors, purple: fluorine, red: oxygen, blue: nitrogen.

subsystem separation r. The pairwise decomposition for the interaction energy gives:

$$E_A(\text{int}) = E_A[e_\text{F}, P_r, r, b] - E_A[(e_p, e_w), P_\infty, \infty, 0] \tag{17}$$

$$E_{AB}'(\text{int}) = E_{AB}'[\epsilon_\text{F}, P_r, r, b] - E_{AB}'[(\epsilon_p, \epsilon_w), P_\infty, \infty, 0] \tag{18}$$

$$E_{AB}(\text{int}) = E_{AB}[\epsilon_\text{F}, P_r, r, b] - E_{AB}[(\epsilon_p, \epsilon_w), P_\infty, \infty, 0] \tag{19}$$

$$E_{\text{core}AB}(\text{int}) = E_{\text{core}AB}[\epsilon_\text{F}, P_r, r, b] - E_{\text{core}AB}[(\epsilon_p, \epsilon_w), P_\infty, \infty, 0] \tag{20}$$

Equations for $E_A(\text{es})$, $E_A(\text{pol})$, $E_A(\text{CT})$ etc. are obtained in a similar manner; of course, $E_{\text{core}AB}(\text{pol}) = E_{\text{core}AB}(\text{CT}) = 0$. It should be stressed that these equations constitute the first nonempirical *pairwise* model for polarization. The only approximations used in eqs 9–12 and 17–20 are the use of a single determinant wave function, and the NNDO approximation. Any other approximation or deficiency stems solely from the Hamiltonian used in the actual implementation (MNDO,[26] AM1,[24] or PM3[25]).

We obtained the X-ray crystal structure coordinates of the nine fluorinated SBB inhibitors bound to HCAII from the PDB.[43] [The structure of unfluorinated SBB complexed with HCAII has not been submitted to the PDB (personal communication with David Christianson.)] The ligands were protonated and divided into three groups or subsystems as depicted in Figure 3. The first subsystem (SS1) comprises the sulfonamide moiety bound to the aromatic ring, the second subsystem (SS2) consists of the peptide unit, and the third subsystem (SS3) encompasses the benzyl group where the fluorine substitutions were made. The protein was divided into subsystems based on standard amino acid residue definitions and also into backbone and side chain groups of the protein chain. QM calculations were performed using DivCon,[23] and the Poisson–Boltzmann (PB) based self-consistent reaction field method[31] (SCRF) was used to obtain the solvated density matrix. We used both the AM1 and PM3 Hamiltonians in these calculations. Pairwise decomposition of the interaction energy between the protein and the ligand subsystems was calculated using the formalism as described above. We note that only the E_{AB} component
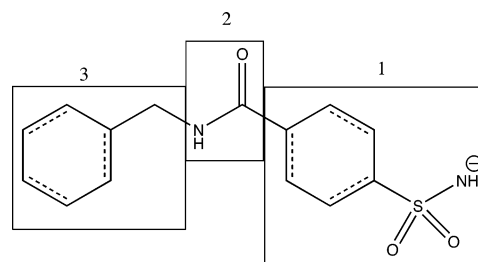

Figure 3. Division of *N*-(4-sulfamylbenzoyl)benzylamine (SBB) into subsystems for the pairwise decomposition analysis. The sulfonamide group in subsystem 3 was modeled as an anion in the complex for pairwise decomposition analysis.

(eq 12) of the pairwise interaction energy was used to study the interaction between subsystems because this term contains most of the binding energy between groups (core–electron and exchange terms).

We also compared semiempirical and Hartree–Fock interaction energies for the T-shaped stacking interaction between benzene and its fluorinated species in this study. We extracted the aromatic ring of the SBB inhibitors (SS3) and the aromatic ring of Phe131 and performed Hartree–Fock geometry optimizations for each of the five ring systems, namely, benzene–benzene, benzene–2-fluorobenzene, benzene–2,3-difluorobenzene, benzene–2,6-difluorobenzene, and benzene–2,3,4,5,6-pentafluorobenzene with the 6-31+G* basis set using the GDIIS (geometry optimization using direct inversion in the iterative subspace) optimization routine.[52,53] The geometries of all of the ring dimer systems maintained an approximate "T" shape when optimized. Interaction energies, ΔE_I, were calculated by doing single-point Hartree–Fock calculations using the counterpoise method to correct for basis set superposition error (BSSE).[54] All Hartree–Fock calculations were performed using Gaussaian 98.[55] To estimate the accuracy of semiempirical methods for calculating interaction energies of ring systems, heats of interaction, ΔH_I, were calculated at the AM1 and PM3 levels of theory for each of the five aromatic ring systems at the optimized Hartree–Fock geometries. These heats of interaction were then

(48) Fischer, H.; Kollmar, H. *Theor. Chim. Acta* **1970**, *16*, 163.
(49) Dewar, M. J. S.; Lo, D. H. *J. Am. Chem. Soc.* **1971**, *93*, 7201–7205.
(50) Olivella, S.; Vilarrasa, J. *J. Heterocycl. Chem.* **1981**, *18*, 1189.
(51) van der Vaart, A.; Merz, K. M., Jr. *J. Phys. Chem. A* **1999**, *103*, 3321–3329.

(52) Farkas, O.; Bernhard Schlegel, H. *J. Chem. Phys.* **1999**, *111*, 10806–10814.
(53) Pulay, P. *J. Comput. Chem.* **1982**, *3*, 556–560.
(54) Simon, S.; Duran, M.; Dannenberg, J. J. *J. Phys. Chem. A* **1999**, *103*, 1640–1643.

compared to the interaction energies calculated using the Hartree–Fock method.

Results and Discussion

Pairwise Interaction between Phe131 and SS3. We calculated the interaction energy between Phe131 and subsystem 3 (SS3) of SBB (see Figure 3) that includes the aromatic ring where the fluorine substitutions were made, using the AM1 and PM3 Hamiltonians. We also calculated the Coulombic interaction energy between Phe131 and SS3 using solvated CM2 atomic charges obtained from the QM calculation and a soft-core Coulombic interaction potential (Raha and Merz, manuscript in preparation). In Table 2A we list the pairwise interaction energy (PW$_{int}$) between Phe131 and SS3 for the five SBB inhibitors complexed with the wild-type HCAII enzyme. The relationship between the QM PW$_{int}$ and the distance between Phe131 and the centroids of the various SS3s is tellingly different when compared to the Coulombic PW$_{int}$. The QM PW$_{int}$ using both the AM1 and PM3 Hamiltonians indicates that substitution of fluorine on the aromatic ring actually favors the interaction between Phe131 and SS3. This is true for 2-fluoro-SBB, 2,3-difluoro-SBB, 2,6-difluoro-SBB, and 2,3,4,5,6-penta-fluoro-SBB where the PW$_{int}$ becomes favorable with incremental fluorination of the aromatic group. This observation is chemically counterintuitive because the higher electronegativity of fluorine should disrupt the edge-to-face interaction between the ring hydrogen atoms of Phe131 and the aromatic group of SBB, leading to less attractive interaction. Indeed, the Coulombic PW$_{int}$ bears this out where substitution of fluorine at position 2 of the aromatic ring actually makes the interaction more repulsive (−0.017 to 0.003 kcal/mol for AM1 based charges). [Due to the absence of the native HCAII–SBB X-ray crystal structure, we *substituted* the fluorine in HCAII–2-fluoro-SBB crystal structure to hydrogen.] Subsequent increase in fluorination of the aromatic ring at positions 2,3, and 2,6, and 2,3,4,5,6 leads to greater repulsion as seen in the Coulombic PW$_{int}$. However, in the X-ray crystal structures the opposite trend is observed that is in agreement with the QM PW$_{int}$, i.e. with increasing fluorination of the aromatic ring the distance, as calculated between the centroid of Phe131 and SS3, decreases (Table 2A). The only exception is for 2,6-difluoro-SBB where the distance between the centroids increases to 6.76 Å, while QM PW$_{int}$ calculates the most favorable interaction, thereby, breaking with the trend. However, a closer look at the X-ray structure of the HCAII–2,6-difluoro-SBB complex reveals that the edge-to-face interaction seen in other inhibitors in not present in this case (Figure 2a). Here the aromatic ring has rotated around the C-phenyl bond to disrupt the edge-to-face interaction to place the fluorine at position 2 of the aromatic group into close proximity to the ring hydrogen of Phe131. This new interaction motif leads to a favorable interaction due to the presence of a partial negative charge on the fluorine and partial positive charge on the hydrogen. This is in fact evidenced in the QM PW$_{int}$ between Phe131 and SS3, which has the most favorable interaction energy for both the AM1 (−1.81 kcal/mol) and PM3 (−4.2 kcal/mol) Hamiltonians. PM3 systematically overestimates the pairwise interaction between the two subsystems for all the inhibitors. It is encouraging that our QM PW$_{int}$ analysis agrees with structural aspects of the binding of SBB inhibitors as seen in the experimental structures.

To probe this aspect of the interaction even further, we divided the amino acid residues into two subsystems. The main chain subsystem consisted of the NH, Cα, and CO groups, whereas the side-chain subsystems encompassed all of the side-chain atoms starting at Cβ. Thus, the Phe131 "residue" in this instance consisted of the Cβ carbon and the phenyl group. The PW$_{int}$ between the side chain of Phe131 and SS3 is essentially identical (RMSD 0.001 kcal/mol) to that between the complete residue and SS3. This validates that this interaction is predominantly an edge-to-face interaction between the aromatic ring of Phe131 and SS3 and is not affected by the backbone.

Regardless of the favorable qualitative results, the relationship between binding affinity and PW$_{int}$ between Phe131 and SS3 for the inhibitors bound to native HCAII only shows a weak *inverse* correlation (see Table 2A). Interestingly, if the modeled parent inhibitor, SBB, is not taken into consideration, then there is a significant *inverse* correlation ($R^2 = 0.7$) between the binding affinity and PW$_{int}$ for the remaining four fluorine-substituted inhibitors. The inverse correlation between binding affinity and PW$_{int}$ in this case implies that stronger PW$_{int}$ between Phe131 and SS3 actually opposes binding. However, we note that there are only four inhibitors in this case, and hence, broad conclusions regarding structure–activity relationships from this observation could be misleading.

There is always an issue regarding the ability of semiempirical methods to model biomolecular interactions, especially hydrogen bonding, correctly.[28,56] Energy decomposition studies done by van der Waart and Merz[51] have shown that Coulombic energies of interaction are generally repulsive and stabilization is due to polarization and charge transfer during interaction. Cummins et al. have argued that this apparent stabilization due to electronic reorganization is artificial because ab initio calculations find that stabilization is predominantly due to the electrostatic part of the interaction.[56] While the accuracy of energy decomposition into electrostatic, polarization, and charge-transfer components using semiempirical methods is the subject of debate, van der Vaart and Merz in subsequent studies have calculated interaction energies at Hartree–Fock (HF) and MP2 levels of theory using various basis sets and shown excellent agreement (R^2 greater than 0.99) between ab initio interaction energies and semiempirical interaction energies for biomolecular model chemistries such as hydrogen-bonding and salt-bridge interactions.[57] In this study we have investigated the T-shaped stacking interactions between benzene and fluorine-substituted benzene rings of the kind seen in protein–ligand interactions and specifically in this set of SBB inhibitors bound to HCAII (see Theoretical Background and Computational Details).

We have listed the interaction energy ΔE_I, calculated with HF/6-31+G*, and heats of interaction ΔH_I, calculated with the

(55) Frisch, M. J.; Trucks, G. W.; Schlegel, H. B.; Scuseria, G. E.; Robb, M. A.; Chesseman, J. R.; Zakrzewski, V. G.; Montgomery, J. A., Jr.; Stratmann, R. E.; Burant, J. C.; Dapprich, S.; Millam, J. M.; Daniels, A. D.; Kudin, K. N.; Strain, M. C.; Farkas, O.; Tomasi, J.; Barone, V.; Cossi, M.; Cammi, R.; Mennucci, B.; Pomelli, C.; Adamo, C.; Clifford, S.; Ochterski, J.; Petersson, G. A.; Ayala, P. K.; Cui, Q.; Morokuma, K.; Malick, D. K.; Rabuck, A. D.; Raghavachari, K.; Foresman, J. B.; Cioslowski, J.; Ortiz, J. V.; Baboul, A. G.; Stefanov, B. B.; Liu, G.; Liashenko, A.; Piskorz, P.; Komaromi, I.; Gomperts, R.; Martin, R. L.; Fox, D. J.; Keith, T.; AlLoham, M. A.; Peng, C. Y.; Nanayakkara, A.; Gonzalez, C.; Challacombe, M.; Gill, P. M. W.; Johnson, B. G.; Chen, W.; Wong, M. W.; Andres, J. L.; Head-Gordon, M.; Replogle, E. S.; Pople, J. A. A.9 ed.); Gaussian Inc.: Pittsburgh, 1998.

(56) Cummins, P. L.; Titmuss, S. J.; Jayatilaka, D.; Bliznyuk, A. A.; Rendell, A. P.; Gready, J. E. *Chem. Phys. Lett.* **2002**, *352*, 245–251.

(57) van der Vaart, A.; Merz, K. M., Jr. *Int. J. Quant. Chem.* **2000**, *77*, 27–43.

Table 3. PW_{int} between Thr199 and SS1 of SBB inhibitors bound to native and F131V mutant of HCAII[a]

complex inhibitor	ΔG_{bind} (kcal/mol)	PW_{int} AM1 (kcal/mol)	PW_{int} PM3 (kcal/mol)	PW_{int} VDW (kcal/mol)	PW_{int} PM3 (kcal/mol)	
					Thr199$_{sc}$-SBB(1)	Thr199$_{bb}$-SBB(1)
native−SBB	−11.80	−32.8	−50.00	−0.91	−31.06	−18.95
native−2-fluoro-SBB	−12.84	−32.94	−50.14	−0.91	−31.20	−18.96
native−2,3-difluoro-SBB	−12.97	−40.63	−59.44	−0.43	−33.63	−25.87
native−2,6-difluoro-SBB	−12.30	−33.26	−50.54	−0.83	−27.51	−23.07
native−pentafluoro-SBB	−12.00	−35.46	−53.23	−0.72	−30.31	−22.96
F131V−SBB	−11.22	−25.35	−39.18	−1.30	−23.04	−16.14
F131V−2-fluoro-SBB	−11.75	−26.35	−41.86	−1.24	−24.49	−17.40
F131V−2,3-difluoro-SBB	−11.96	−24.45	−39.27	−1.36	−16.93	−22.40
F131V−2,6-difluoro-SBB	−11.44	−22.85	−36.69	−1.36	−17.25	−19.48
F131V−pentafluoro-SBB	−11.83	−18.06	−30.76	−1.58	−13.62	−17.18

[a] PW_{int} calculated using AM1 and PM3 Hamiltonian, and van der Waals interaction has been listed for 10 SBB inhibitors bound to HCAII. The PW_{int} is further divided into the backbone (Thr199$_{bb}$)PW_{int} and side chain (Thr199$_{sc}$)PW_{int} of Thr199. The key interactions between SBB(1) and Thr199$_{bb}$ is a hydrogen bond between the sulfonamide oxygen and backbone NH of Thr199, and a side chain OH of Thr199 and NH from sulfonamide group (see Figure 5).

semiempirical AM1 and PM3 Hamiltonians, in Table 2B. AM1 and PM3 systematically underestimate the absolute interaction energy between these aromatic dimers (AM1 more than PM3), but the trend between the interaction energies (ab initio) and enthalpies (semiempirical) are in excellent agreement (R^2 of 0.97 between ΔE_I and ΔH_I for AM1 and R^2 of 0.98 between ΔE_I and ΔH_I for PM3). The intracentroid distances between the aromatic rings are also listed in Table 2B. The Hartree−Fock optimized geometries suggest that the fluorination of benzene leads to a decrease in the distances between the centroids of the aromatic rings, whereas the interaction is less favorable than that between two benzene rings in a T-shaped stack. This is in contrast to our observation of the distances in the X-ray crystallographic structures of SBB inhibitors bound to HCA II and the pairwise interaction energies calculated between Phe131 and SS3. While the distances between the centroids of Phe131 and SS3 decrease with increase in fluorination, the PW_{int} also becomes more favorable (Table 2A).

However, it is not appropriate to compare the two since the geometries on which the calculations are being performed are different. The PW_{int}'s are calculated in the X-ray crystal structure geometries in the presence of the protein environment, whereas the aromatic rings are the geometries as a result of optimization using HF/6-31+G* method. Moreover, the PW_{int}'s represent one pairwise term involved in the total interaction energy, while the ab initio energies are total energies. Within the scope of this study, it suffices to say that the HF/6-31+G* interaction energies correlate well with semiempirical interaction energies calculated for the same geometries. This implies that semiempirical calculations are reliable at least at the level of HF for estimating stacking interactions. In future studies we will systematically investigate such interactions at various levels of theory.

Pairwise Interaction Between Thr199 and SS1. We also investigated the interaction between Thr199 and the sulfonamide group of the SBB inhibitors (subsystem 1 − SS1) using our pairwise decomposition scheme. SS1 includes the aromatic group that is bonded to the sulfonamide moiety (Figure 3). The sulfonamide group profoundly influences the binding affinity of the HCAII inhibitors and functional groups that influence the acidity of the sulfonamide functionality modulates the binding affinity of the inhibitor. For example, $CH_3SO_2NH_2$ inhibits HCAII at 3 mM, whereas the more acidic $CF_3SO_2NH_2$ inhibits HCAII at nanomolar concentrations.[1,42] As described previously, the sulfonamide group interacts with Thr199, a

residue which plays a role in catalysis,[41] by making a strong hydrogen bond between the NH group and the side chain hydroxyl group of Thr199. The importance of this interaction has been discussed in the literature, and Thr199 is often considered as a "doorkeeper" to the active site as it only accepts anions capable of donating a hydrogen bond to the side chain hydroxyl group of Thr199.[47] In Table 3 we list the QM and Coulombic PW_{int} between Thr199 and SS1. The first very obvious observation from Table 3 is the strength of the PW_{int} between Thr199 and SS1 of the SBB inhibitors. This interaction is approximately an order of magnitude stronger than the interaction between Phe131 and SS3. The strength of the interaction calculated using the PM3 Hamiltonian is stronger than that calculated using the AM1 Hamiltonian. The square of the correlation coefficient (R^2) between the AM1 PW_{int} and PM3 PW_{int} is 0.99, implying that PM3 systematically overestimates (or AM1 underestimates) the pairwise interaction energy between the two subsystems. However, some of the most interesting and striking observations between the PW_{int}'s for these two subsystems are their relationship to the binding affinity of the SBB inhibitors. AM1 PW_{int} correlates with the binding affinity of the inhibitors with an R^2 of 0.5 (RMSD 0.37 kcal/mol) whereas the PM3 PW_{int} correlates with an R^2 of 0.51 (RMSD 0.37 kcal/mol). This is a very good agreement between binding affinity and PW_{int}, considering that we are only calculating the interaction between two subsystems out of the *entire* complex. Also, the range of the free energy of binding for these 10 inhibitors is just 1.75 kcal/mol.

It should be kept in mind that due to the absence of the X-ray crystal structure of SBB bound to native HCAII we modeled it by substituting the fluorine on 2-fluoro-SBB with a hydrogen. The protons on the modeled structure were geometry optimized with the heavy atoms fixed, using the AMBER96[14] force field along with the other protein−ligand complexes in this study. While this structure still involves an edge-to-face interaction between the two aromatic rings, the positioning of the centroids of the phenyl rings is slightly different (0.03 Å), which will introduce some error in the computed PW_{int} value. Furthermore, for the complex between 2,3,4,5,6-pentafluoro-SBB and the F131V mutant of HCAII, 2:1 inhibitor binding was observed in the X-ray crystal structure. Kim et al. suggest that in solution, however, a single inhibitor molecule binds to HCAII, leading to some uncertainty in calculating the binding affinity from the crystal structure.[44] Hence, if the binding affinities of the other eight inhibitors (without SBB bound to HCAII, and 2,3,4,5,6-
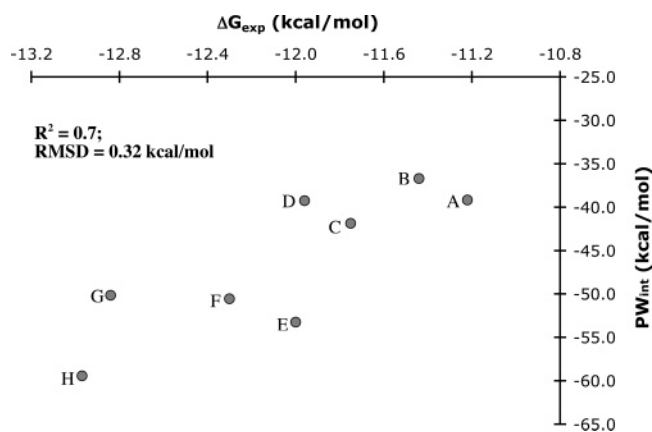
Figure 4. PM3 PW_{int} between Thr199 and SS1 and its relationship to the binding affinity of eight inhibitors. The square of the correlation coefficient is 0.7 with an RMSD of 0.32 kcal/mol between PW_{int} and ΔG_{exp}. The protein−ligand complexes corresponding to letters in the figure are: **A**: F131V−SBB, **B**: F131V−2,6-difluoro-SBB, **C**: F131V−2-fluoro-SBB, **D**: F131V−2,3-difluoro-SBB, **E**: native−pentafluoro-SBB, **F**: native−2,6-difluoro-SBB, **G**: native−2-fluoro-SBB, **H**: native−2,3-difluoro-SBB.

Figure 5. Hydrogen bond interactions between Thr199 and SS1 of SBB. Thr199 residue has two key hydrogen bond interactions with SS1 of SBB: backbone NH with Oxygen of the sulfonamide moiety, and the side chain OH with NH of the sulfonamide moiety. The H-bonding distance in Å for inhibitors bound to HCAII and inhibitors bound to mutant F131V HCAII are depicted in that order. Color code, **black**: 2-fluoro-SBB, **red**: 2,3-difluoro-SBB, **green**: 2,6,-difluoro-SBB, **blue**: 2,3,4,5,6-pentafluoro-SBB.

pentafluoro-SBB bound to F131V CA II) are compared with PW_{int}, we obtain better agreement with experiment with a R^2 of 0.67 (RMSD, 0.33 kcal/mol) for the AM1 Hamiltonian and a R^2 of 0.7 (RMSD, 0.32 kcal/mol) for the PM3 Hamiltonian (Figure 4). This observation has several implications. The sulfonamide group (SS1) is identical in all of the inhibitors in terms of its chemical composition, and the only difference between the inhibitors in this group is their 3-D structures. On the other hand, although the interaction between SS3 and Phe131 is *inversely* correlated with binding affinity (see Table 2), in the absence of the F131−SS3 interaction, conclusions cannot be drawn for the complete dataset. For inhibitors bound to the F131V HCAII mutant, the PW_{int} calculated between SS3 and V131 is zero. Also we note again that, in terms of the magnitude of the interactions themselves, the SS3−Phe131 interaction is a lot weaker than the SS1−Thr199 interaction (see Table 3). Hence, while it appears that fluorination of the aromatic ring of the base SBB inhibitor modulates binding affinity weakly due to the strength of the interaction, we conclude that it impacts binding affinity by altering the positioning of the sulfonamide group and influencing the dominant interaction between the sulfonamide group and the Thr199 residue. We note that the importance of the positioning of the sulfonamide group in the HCAII−substrate complex was noted in an early study of King and Burgen.[58] They formulated a two-step kinetic model to explain the effects of different substituents on position 4 of benzene sulfonamides bound to human carbonic anhydrase. On the basis of their experimental observations, King and Burgen concluded, "It seems likely that the stability of the complex depends mainly on the coordination energy of the metal−sulfonamide bond and that other structural features are mainly concerned with the steric placing of the sulfonamide."

Decomposition of Thr199-SS1 Interaction into Side-Chain and Backbone Interactions. The interaction between SS1 and Thr199 can be divided into two important hydrogen-bonding interactions (see Figure 5). One of them is the interaction of the hydrogen bonded to the sulfonamide nitrogen with the side-chain hydroxyl (OH) group of Thr199. The other interaction is
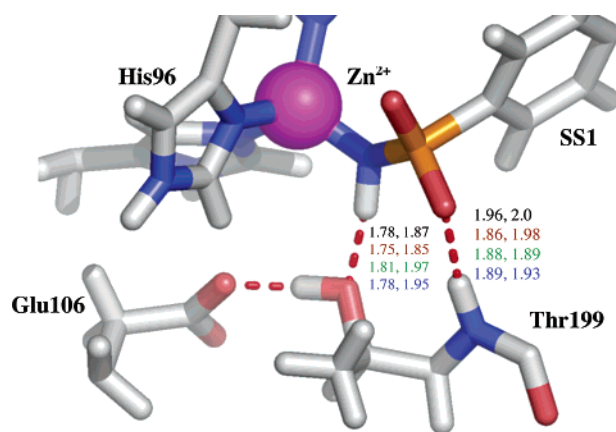
(58) King, R. W.; Burgen, A. S. V. *Proc. R. Soc. London, Ser. B* **1976**, *193*, 107−125.

the hydrogen bond between the sulfonamide oxygen and the backbone NH of Thr199. These hydrogen-bonding distances are listed in Figure 5. To probe this interaction even further, we carried out a pairwise decomposition analysis where Thr199 was divided into two subsystems consisting of the backbone ($Thr199_{bb}$) and the side-chain ($Thr199_{sc}$) groups. Since we get better agreement with experimental binding free energies using the PM3 Hamiltonian, we will focus our discussion only on the PM3 PW_{int} results for the sake of brevity. One obvious conclusion from this analysis is that the strength of interaction between SS1 and $Thr199_{sc}$ is stronger than between $Thr199_{bb}$ and SS1 for the inhibitors bound to native HCAII (Table 3). This is in agreement with the structure of the protein−inhibitor complexes in terms of the hydrogen-bonding distance between the side-chain and backbone groups of Thr199 with SS1 (Figure 5). For the inhibitors bound to HCAII, the average distance between the Thr199 backbone hydrogen (NH) and the sulfonamide oxygen is 1.94 Å, and the distance between hydrogen bonded to sulfonamide nitrogen and side-chain oxygen (hydroxyl group) of Thr199 is 1.78 Å. For inhibitors bound to the F131V mutant, the average distances are 1.95 and 1.94 Å, respectively. As expected, the sum of $Thr199_{sc}$ PW_{int} and $Thr199_{bb}$ PW_{int} approximately equals the PW_{int} between the entire Thr199 residue and SS1, which demonstrates the pairwise nature of our scheme.

Subsystem interactions were calculated as a sum of atomic pairwise interactions belonging to a particular subsystem (see Computational Details). This decomposition, however, allows us to assess, for example, the percent contribution of the backbone and side-chain "groups" toward binding. On average, 58% of the interaction between Thr199 and SS1 for inhibitors bound to HCAII is due to $Thr199_{sc}$, and 42% of it is due to $Thr199_{bb}$. For inhibitors bound to mutant F131V HCAII, on average both $Thr199_{sc}$ and $Thr199_{bb}$ contribute equally (50%) toward this interaction. Interestingly, the relationship between the binding affinity of the inhibitors and the PW_{int} of $Thr199_{bb}$ and $Thr199_{sc}$ reveals that neither of the two interactions influences the binding affinity more than the total interaction between the entire Thr199 residue and SS1. The R^2 between the experimental binding free energy of the eight inhibitors and

Table 4. PW$_{int}$ between Pro202 and SS3 of SBB Inhibitors Bound to Native and the F131V Mutant of HCAII[a]

complex inhibitor	ΔG_{bind} (kcal/mol)	Pro202-SS3 distance (Å)	AM1 PW$_{int}$ (kcal/mol)	PM3 PW$_{int}$ (kcal/mol)	VDW PW$_{int}$ (kcal/mol)
native−SBB	−11.80	4.94	−0.36	−1.37	−1.08
native−2-fluoro-SBB	−12.84	5.16	−0.35	−1.36	−1.1
native−2,3-difluoro-SBB	−12.97	5.75	−0.78	−2.85	−0.90
native−2,6-difluoro-SBB	−12.30	4.79	−3.09	−7.26	−1.49
native−pentafluoro-SBB	−12.00	6.53	−0.14	−0.49	−0.74
F131V−SBB	−11.22	4.82	−1.25	−3.66	−1.49
F131V−2-fluoro-SBB	−11.75	4.95	−1.04	−3.04	−1.36
F131V−2,3-difluoro-SBB	−11.96	5.05	−0.48	−1.64	−1.34
F131V−2,6-difluoro-SBB	−11.44	4.88	−1.72	−4.50	−1.51
F131V−pentafluoro-SBB	−11.83	5.14	−0.29	−1.09	−0.74

[a] PW$_{int}$ calculated using AM1 and PM3 Hamiltonian, and van der Waals interaction has been listed for 10 SBB inhibitors.

PW$_{int}$ for Thr199$_{sc}$ is 0.56, and that for Thr199$_{bb}$ is 0.41, whereas R^2 between entire Thr199 and subsystem 1 for the eight inhibitors is 0.7.

Acidity of the Sulfonamide Group. The acidity of the sulfonamide group has been discussed as an important factor contributing to the binding affinity. In the SBB inhibitors Kim et al. also discussed the inductive effect due to fluorine atoms on the acidity of the sulfonamide group. In their experimental measurements of the pK_a of SBB and 2,3,4,5,6-pentafluoro-SBB, they do not notice any significant perturbation of pK_a values due to fluorination.[44] To further understand how the acidity of the sulfonamide moiety is affected due to fluorination, we calculated the atomic charges on the sulfonamide moiety when bound to different (R) groups. Atomic charges calculated using electronic structure theory contain information about the local environment around an atom.[20] We calculated the CM2[59] atomic charges in water on the sulfonamide atoms in $CH_3SO_2NH_2$, $CF_3SO_2NH_2$, and the five SBB inhibitors using both the AM1 and PM3 Hamiltonians and our PB/SCRF method where the solvent is modeled as uniform dielectric of 80.0.[31] In Table 1 of Supporting Information, we list the charges calculated using the PM3 Hamiltonian, on the atoms of the sulfonamide moiety with different R groups. These calculations are qualitatively in agreement with experimental observations. For example, the nitrogen atom loses electron density (-0.05 e$^-$) due to inductive effects that arise when the methyl hydrogen atoms are replaced by fluorine atoms in $CH_3SO_2NH_2$. Hence, we would predict that the amine group of $CF_3SO_2NH_2$ is less basic (more acidic), which is the case. Alternatively, fluorine substitution on the more distant benzyl group of the SBB inhibitors does not result in significant gains or losses of electron density from the nitrogen atom and, hence, does not affect the acidity of the sulfonamide group (see Table 1 of Supporting Information).

Pairwise Interaction between Pro202 and SS3. Another interaction we sought to probe was that between Pro202 and the fluorine-substituted SBB inhibitors. Due to the nonpolar nature of the Pro202 side chain, the interaction with the fluorine-substituted aromatic ring of the SBB inhibitors is a dipole-induced dipole-type interaction.[44] The range of distances between the Pro202 centroid and the aromatic ring of SBB is 4.94−6.53 Å for inhibitors bound to wild-type HCAII and 4.82−5.14 Å for inhibitors bound to the F131V mutant. However, the PW$_{int}$ between valine 131 in F131V and SS3 is negligible which is also reflected in the separation between the two groups

in the structures. Thus, it appears that in the absence of the dominant interaction between Phe131 and the aromatic ring of SBB, the interaction between Pro202 and the aromatic ring assumes importance. This is also reflected in the relationship between the binding affinity of the inhibitors bound to the mutant and the calculated PW$_{int}$. The R^2 between the Pro202 and SS3 PW$_{int}$ and binding affinity for the inhibitors bound to native HCAII is close to zero, whereas the R^2 for inhibitors bound to the F131V mutant is 0.6 for AM1 and 0.67 for the PM3 Hamiltonian. The average distance between the SS3 and Pro202 is 5.4 Å in HCAII, whereas it is 4.9 Å in the mutant F131V HCAII. Strikingly there is almost a perfect correlation between the distance between Pro202 and SS3 and binding affinity (Table 4) for inhibitors bound to F131V HCAII ($R^2 = 0.97$), whereas for inhibitors bound to native HCAII, it is very weak ($R^2 = 0.13$). Clearly, we find that these interactions between the fluorinated rings of SBB derivatives and Phe131 (Table 2) and Pro202 (Table 4) residues modulate the binding affinity of the inhibitors. However, in terms of sheer magnitude they are lot weaker when compared to the interaction between SS1 and Thr199. However, these weak interactions affect the positioning of SS1 relative to Thr199, and this appears to have the most significant affect on the observed binding affinity.

Given the importance of the interaction between Thr199 and the sulfonamide group of the inhibitors (SS1) and the interaction between Phe131 and SS3, we fit these PM3 PW$_{int}$ (Phe131-SS3, Pro202-SS3, and Thr199-SS1) to experimental ΔG's using multiple linear regression for the eight inhibitors. In this analysis, we achieved an R^2 of 0.75 with an RMSD of 0.27 kcal/mol between the calculated and experimental ΔG of binding (Figure 6). This is a very good agreement and suggests that by combining dominant pairwise interactions between the protein and the ligand we can explain the observed variations in binding affinity. Overall, we find it to be quite revealing that quantum mechanically calculated pairwise electrostatic interaction energies calculated for just a few groups account for such a large portion of the variation in the free energy of binding.

Solvation Free Energy of Complexation. It is well-known that solvent plays a major role in protein−ligand interaction.[2,17,60−62] We have not explicitly considered any solvent effects such as ligand or receptor desolvation in these calculations. It should be kept in mind, though, that the pairwise interaction was calculated from a solvated density matrix

(59) Li, J. B.; Zhu, T. H.; Cramer, C. J.; Truhlar, D. G. *J. Phys. Chem.* **1998**, *102*, 1820−1831.

(60) Eisenberg, D.; McLachlan, A. D. *Nature* **1986**, *319*, 199−203.
(61) Schwarzl, S. M.; Tschopp, T. B.; Smith, J. C.; Fischer, S. *J. Comput. Chem.* **2002**, *23*.
(62) Zou, X.; Sun, Y.; Kuntz, I. D. *J. Am. Chem. Soc.* **1999**, *121*, 8033−8043.
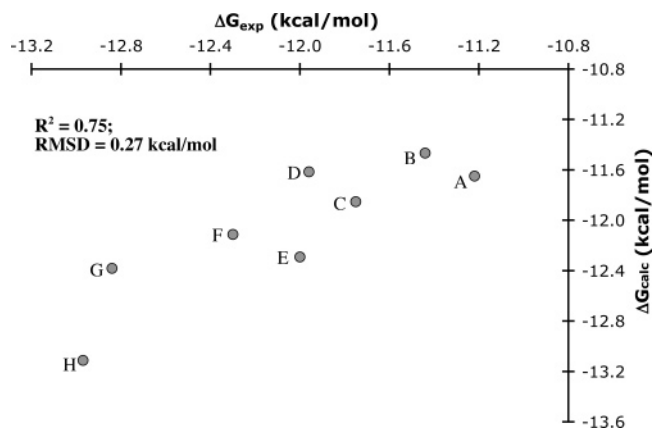
Figure 6. PM3 PW_{int} between Phe131 and SS3, Pro202 and SS3, and Thr199 and SS1 fit to the experimental free energy of binding for eight inhibitors bound to native and mutant HCAII. R^2 for the fit is 0.75 and RMSD between calculated and experimental ΔG is 0.27 kcal/mol. The protein−ligand complexes corresponding to letters in the figure are: **A**: F131V−SBB, **B**: F131V−2,6-difluoro-SBB, **C**: F131V−2-fluoro-SBB, **D**: F131V−2,3-difluoro-SBB, **E**: native−pentafluoro-SBB, **F**: native−2,6-difluoro-SBB, **G**: native−2-fluoro-SBB, **H**: native−2,3-difluoro-SBB.
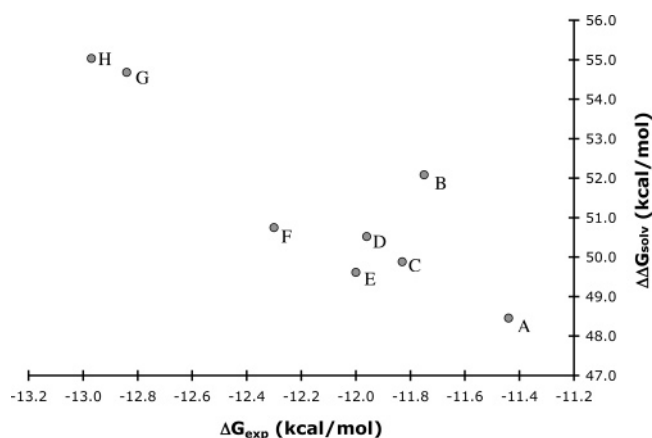

Figure 7. Solvation free energy of complexation for eight fluorine-substituted SBB inhibitors bound to HCAII and mutant F131V HCAII calculated using the PB/SCRF method and PM3 Hamiltonian. The R^2 between $\Delta\Delta G_{solv}$ and ΔG_{exp} of binding is 0.78. The protein−ligand complexes corresponding to the letters in the figure are: **A**: F131V−2,6-difluoro-SBB, **B**: F131V−2-fluoro-SBB, **C**: F131V−pentafluoro-SBB, **D**: F131V−2,3-difluoro-SBB, **E**: native−pentafluoro-SBB, **F**: native−2,6-difluoro-SBB, **G**: native−2-fluoro-SBB, **H**: native−2,3-difluoro-SBB.

obtained from a PB/SCRF calculation. Hence, the effect of solvent is implicitly included in the pairwise decomposition itself. We also explicitly calculated the cost of desolvation of the inhibitor and the receptor using the following expression:

$$\Delta\Delta G_{solv} = \Delta G_{solv}^{PI} - \Delta G_{solv}^{P} - \Delta G_{solv}^{I}$$

where $\Delta\Delta G_{solv}$ is the solvation free energy of complexation that includes inhibitor as well as receptor desolvation, ΔG_{solv}^{PI} is the solvation free energy of the protein−inhibitor complex, ΔG_{solv}^{P} is the solvation free energy of the protein, and ΔG_{solv}^{I} is the solvation free energy of the ligand. Solvation free energies were calculated using the AM1 and PM3 Hamiltonians and CM2 charges using our PB/SCRF.[31] Interestingly, we found $\Delta\Delta G_{solv}$ to be *inversely* correlated with the binding affinity of the fluorine-substituted inhibitors (Figure 7). For the PM3 Hamiltonian we obtain R^2 of 0.78 (Figure 7), and for AM1 we obtain R^2 of 0.84 (Figure 1, Supporting Information) between $\Delta\Delta G_{solv}$

and ΔG_{exp} for eight fluorine-substituted SBB inhibitors bound to HCAII and mutant F131V HCAII, respectively. This is an excellent agreement, considering that the range of the binding free energy is just 1.75 kcal/mol and the solvation free energy is calculated from one single structure of the protein−inhibitor complexes. The desolvation penalty paid by the receptor and the ligand due to complex formation is inversely related to the free energy of binding, which is expected. We find that the parent SBB inhibitor bound to HCAII and the F131V mutant are outliers in this case. The solvation free energy of complexation for SBB bound to HCAII is 64.7 kcal/mol and that for SBB bound to F131V mutant is 66.6 kcal/mol; however, they break with the trend of correlating with binding affinity. It can be argued that the SBB−HCAII complex was a modeled structure and thus not well suited for our structure-based estimation of the desolvation cost, but it is not clear why F131V HCAII−SBB complex is an outlier. Barring these outliers, this analysis reveals the importance of desolvation of the ligand and the receptor in determining the free energy of binding. The pairwise interaction energies between different subsystems of the protein and the ligand have a direct relationship with ΔG_{exp}, whereas the desolvation due to complexation is inversely correlated with experimental binding affinity. This observation implies that the free energy of binding is a fine balance between the enthalpic interactions between the protein and ligand atoms in the active site and the desolvation cost paid by receptor and the ligand due to complexation. Notably, the strength of the interaction between SS3 and Thr199 is approximately on the same scale as the desolvation penalty paid by the receptor and the ligand. Thus, it appears that variation in the binding free energy, which is of the order of few kcal/mol, is a sum of the two large opposing forces.

Conclusions

In this study we have described the theoretical and computational aspects of a semiempirical pairwise decomposition scheme that can be used to calculate the pairwise interaction between two molecules. The advent of linear scaling QM technology makes it possible to study protein−ligand interaction using QM approaches without having to resort to approximations utilized in molecular mechanical models (e.g., fixed atomic charges, etc.). Making use of our linear scaling divide and conquer method, we have used this pairwise decomposition scheme to study the interaction of inhibitors bound to the enzyme HCAII and understand the structure−function relationships which cannot be probed experimentally. This system was well suited for such a study because of the well-controlled experimental design and the availability of structure−activity data in the literature. Some of the conclusions from this study regarding the effect of substitution of fluorine in the aromatic ring of the inhibitors were counterintuitive and highlight the subtle interplay between structure and activity. We observed that fluorine substitution, rather than directly affecting binding affinity by its interaction with the Phe131 of HCAII, does so indirectly by influencing the interaction between the sulfonamide groups of the inhibitors and the enzyme. Binding affinity is highly correlated with the strongest interaction between the sulfonamide group and the Thr199 residue in the enzyme and is influenced both by its electronic and structural aspects. This observation validates an early experimental study that under-

scored the importance of the "steric placement" of the sulfon-amide moiety in binding to human carbonic anhydrase.[58] We have also shown the importance of solvation/desolvation effects in this study. The solvation free energy due to complexation is inversely related to the binding affinity of the ligands. Thus, desolvation penalties paid by the receptor and ligand oppose binding but are compensated by strong enthalpic interaction in the active site between the ligand and the protein atoms.

Although these are semiempirical calculations, it is clear that QM methods capture higher-order effects such as polarization and charge transfer that cannot be captured using molecular mechanics potentials, as shown elsewhere in the literature.[63,64] Admittedly, high-level ab initio or density functional methods would be more accurate, but such calculations are intractable at the present time. This study also demonstrates the utility of using linear scaling QM methods to understand aspects of protein−ligand interaction that can be used in rational drug design. Computational methods are increasingly playing im-portant roles in all stages of drug discovery.[65−67] Our pairwise decomposition scheme could be easily applied to the late-stage process of drug discovery wherein submicromolar leads from a high throughput screening experiment have to be optimized for potency. In some regards this study also shows the impact of subtle structural changes on binding affinity. Docking potentials that try to predict the correct binding mode have to overcome this challenge to be successful. This bolsters the case for development of more accurate and physically based docking potentials for enrichment in *in silico* high throughput data-base screening experiments.[68−70] This is true especially when metal ions are involved in the interaction between the protein and the inhibitor and steric and when electrostatic aspects of the metal binding site determine binding affinity. In future work we hope to demonstrate this further by applying our methods to other proteins that are targets for structure-based drug design efforts.

Supporting Information Available: Table 1: Solvated CM2 charges on atoms of the sulfonamide moeity bonded to various R groups; Figure 1: Solvation free energy of complexation for eight fluorine-substituted SBB inhibitors calculated using the PB/SCRF method and AM1 Hamiltonian. This material is available free of charge via the Internet at http://pubs.acs.org

JA042666P

(63) Garcia-Viloca, M.; Truhlar, D. G.; Gao, J. *J. Mol. Biol.* **2003**, *372*, 549−560.
(64) van der Vaart, A.; Merz, K. M., Jr. *J. Am. Chem. Soc.* **1999**, *121*, 9182−9190.
(65) Cheng, A.; Diller, D.; Dixon, S.; Egan, W.; Lauri, G.; Merz, K. M., Jr. *J. Comput. Chem.* **2002**, *23*, 172−183.
(66) Kuntz, I. D. *Science* **1992**, *275*, 1078−1082.
(67) Jorgensen, W. L. *Science* **2004**, *303*, 1813−1818.
(68) Waszkowycz, B. *Curr. Opin. Drug. Discovery Dev.* **2002**, *5*, 407−413.
(69) Perez, C.; Ortiz, A. R. *J. Med. Chem.* **2001**, *44*, 3786−3785.
(70) Taylor, R.; Jewsbury, P. J.; Essex, J. W. *J. Comput.-Aided. Mol. Des.* **2002**, *16*, 151−166.